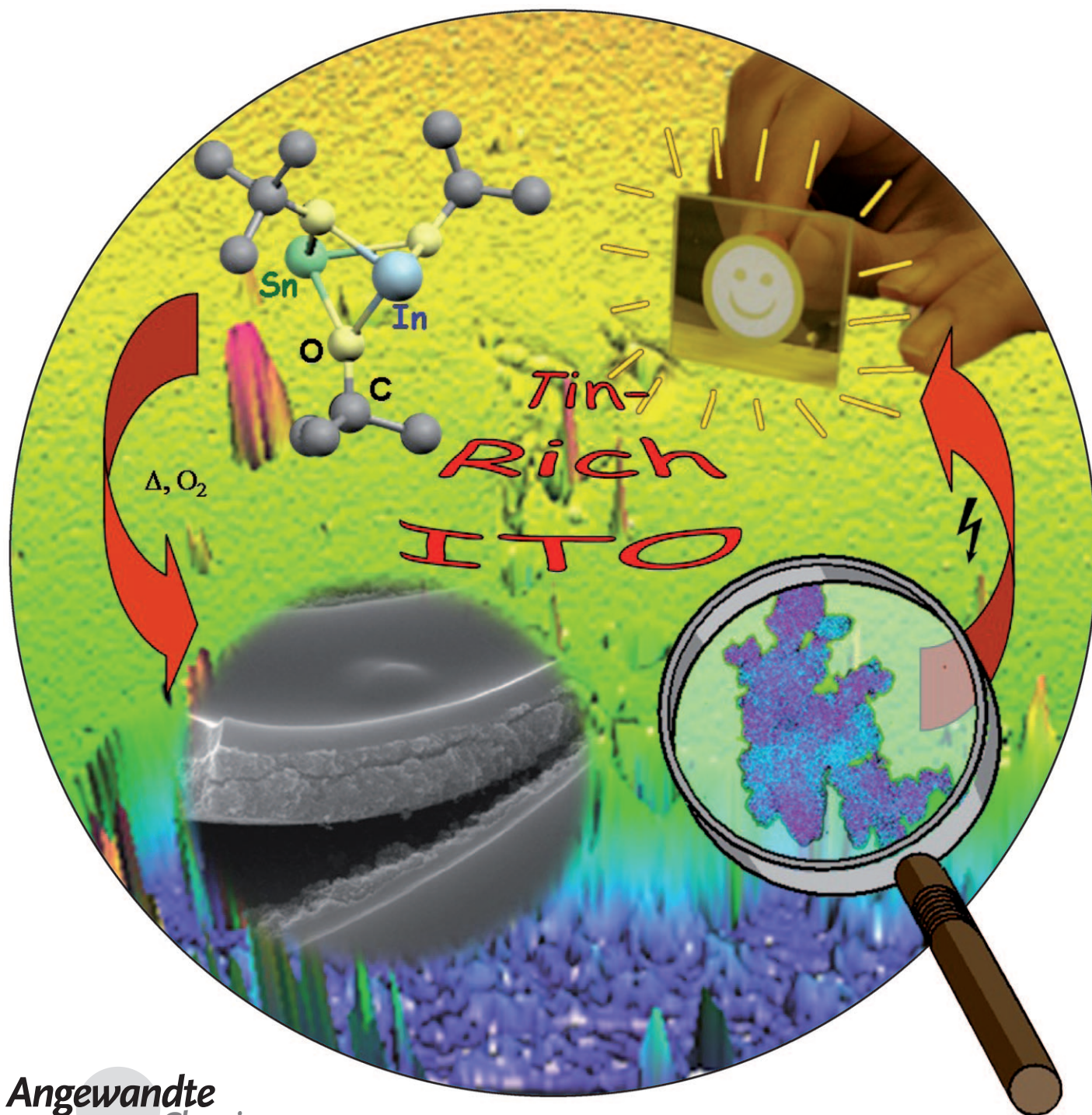


# A Low-Temperature Molecular Approach to Highly Conductive Tin-Rich Indium Tin Oxide Thin Films with Durable Electro-Optical Performance\*\*

Yilmaz Aksu and Matthias Driess\*



Angewandte  
Chemie

Currently, many optoelectronic devices such as transparent electrodes in flat-panel technology,<sup>[1]</sup> organic light-emitting diodes (OLEDs), and photovoltaics<sup>[2]</sup> rely on transparent conducting oxides (TCOs). Indium tin oxide (ITO;  $\text{In}_2\text{O}_3\cdot\text{Sn}$  doped with 5–15 mol %  $\text{Sn}^{\text{IV}}$ ) is one of the most widely applied TCOs with very good performance in terms of electrical conductivity, high transparency in the visible range, and high reflectivity in the near-IR region for energy-saving windows.<sup>[3]</sup> It is typically utilized as a thin film on glass supports and can be applied by various methods, including gas-phase deposition techniques.<sup>[4]</sup> Recently, for many reasons including cost effectiveness, liquid-phase processing of ITO thin films, prepared from highly crystalline uniform nanoparticles (or colloids), has become an alternative for certain applications.<sup>[5,6]</sup>

Thus, ITO nanoparticles suitable for wet deposition techniques, such as spin- and dip-coating, are commonly accessible by wet-chemical approaches under mild conditions, which apply co-precipitation and subsequent chemical and/or thermal post-treatment.<sup>[7]</sup> Although co-precipitation can lead to uniform crystalline ITO nanoparticles with Sn-dopant concentrations from 1 to 13 mol %, <sup>[5,6]</sup> it is difficult to adjust homogeneous compositions.

Nevertheless, ITO nanocrystals with about 8 mol % Sn can even be employed for low-cost printing techniques on flexible and heat-sensitive substrates such as plastics.<sup>[6]</sup> The field of printable electronics represents another fast-growing area of ITO applications.<sup>[6,8]</sup> However, the growing demand for ITOs, combined with the relatively low natural abundance of indium, generates a bottleneck and leads to high production costs.

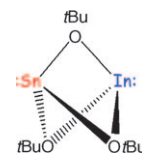
Alternative TCO materials, such as Al:ZnO (AZO) films,<sup>[9]</sup> are much cheaper, but their conductivity is significantly lower (by about four times) than that of ITO. A notable improvement would be to gain access to tin-rich ITO substrates with a tin content much larger than 15 mol % without significant loss of the high conductivity and transparency of the best ITO materials utilized in optoelectronic devices. Current studies have shown that the solubility limit of Sn in  $\text{In}_2\text{O}_3$  depends on the particle size and temperature.<sup>[10]</sup> Previous attempts to prepare tin-rich ITO samples by sintering at 1550 °C failed and led merely to the poorly conducting rhombohedral  $\text{In}_4\text{Sn}_3\text{O}_{12}$  phase.<sup>[11]</sup> To avoid  $\text{In}_2\text{O}_3/\text{SnO}_2$  segregation of tin-rich ITO, a low-temperature approach with high control over the In/Sn molar ratio is required. Our previous experience with single-source molec-

ular precursors to form predetermined molecular semiconducting heterobimetallic oxides<sup>[12–14]</sup> led us to investigate new ITO materials with high tin content using tin indium alkoxide precursors that are soluble in organic solvents. The use of molecular single-source precursors containing tin and indium in a well-defined molar ratio could facilitate the formation of tin-rich ITO composites with identical stoichiometry in the final product.

To our knowledge, the preparation of ITO materials from a molecular single-source precursor has not yet been reported. Herein we describe the surprisingly facile low-temperature access to the first tin-rich ITO composite with an overall In/Sn ratio of 1:1. This highly conductive and transparent material is synthesized using a single-source heterobimetallic alkoxide precursor (indium tin *tert*-butyl oxide (ITBO); Scheme 1). This precursor is suitable for the preparation of homogeneous and atomically flat ITO composite films on glass substrates, which show an intriguing high performance in energy-saving electroluminescent lamp applications.<sup>[15]</sup> The ITBO precursor is a pale yellow crystalline solid that is accessible in multigram scale through an improved literature procedure.<sup>[16]</sup> It is a nonvolatile, heterobimetallic *tert*-butyl oxide that is highly soluble in hydrocarbons and which assembles with a Sn/In molar ratio of 1:1.

First, the decomposition of ITBO was studied in dry synthetic air (20 %  $\text{O}_2$ , 80 %  $\text{N}_2$ ) under thermogravimetric and derivative thermogravimetric conditions (Figure 1).

Thermogravimetric analysis (TGA) and differential thermogravimetry (DTG) reveal that the main degradation process occurs in the temperature range 100–400 °C, where the combustion of the alkoxide groups takes place. This combustion is associated with one exothermic peak on the DTG curve at  $T = 185^\circ\text{C}$ , thus indicating that decomposition proceeds in only one step. Concomitantly, a rapid loss in mass is observed that reaches –39.7 % at  $T = 400^\circ\text{C}$ . This finding is in accordance with the calculated mass for the organic component in  $\text{In}(\text{tBuO})_3\text{In}$  (38.9 %) and thus indicates that the organic groups have been completely thermally decomposed. The  $^{13}\text{C}$  magic-angle spinning (MAS) solid-state NMR, FTIR, and X-ray photoelectron (XPS) spectra confirm that



**Scheme 1.** The single-source precursor alkoxide ITBO.

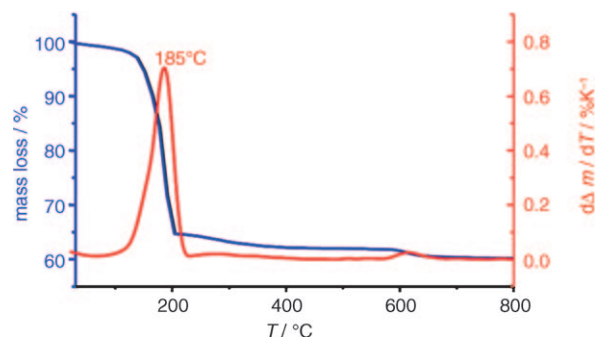


**Figure 1.** TGA and DTG curves for the degradation of the precursor ITBO in dry synthetic air. Heating rate  $1\text{ K min}^{-1}$  from room temperature to 800 °C

[\*] Dr. Y. Aksu, Prof. Dr. M. Driess  
Institute of Chemistry: Metalorganics and Inorganic Materials  
Technische Universität Berlin  
Sekt. C2, Strasse des 17. Juni 135, 10623 Berlin (Germany)  
E-mail: matthias.driess@tu-berlin.de

[\*\*] The authors acknowledge Evonik Degussa GmbH, Marl for cooperation and fruitful discussion, in particular with Dr. Anna Prodi-Schwab, and for financial support. This project of the Science-to-Business Center Nanotronics was cofinanced by the European Union and supported by the state of North Rhine–Westphalia (Germany).

Supporting information for this article is available on the WWW under <http://dx.doi.org/10.1002/anie.200901204>.



the samples prepared at 400 °C are free of the ITBO precursor and organic impurities.

The low decomposition temperature and high organic solubility of ITBO allow processing under fairly mild conditions directly from a solution of the precursor to form highly conductive tin-rich ITO thin films with remarkable long-term stability. Thin-film formation was performed by spin-coating glass under inert conditions using ITBO in toluene, without any additives or stabilizers, and subsequent thermal treatment of the layers in dry synthetic air at both 250 and 400 °C. Because ITO films post-treated with dihydrogen can show a lower electrical resistivity owing to an increase of the carrier concentration,<sup>[21]</sup> the samples were subsequently annealed at their corresponding drying temperature (250 or 400 °C) in a reductive gas mixture (10% H<sub>2</sub>, 90% N<sub>2</sub>) to improve the electro-optical properties of the tin-rich ITO layers. Remarkably, the starting ITBO layers are very homogeneous and, after thermal treatment, lead to very compact tin-rich ITO films with strikingly flat morphology (Figure 2). As confirmed by SEM imaging, the tin-rich ITO coatings are highly amorphous. Correspondingly, transmission electron microscopy (TEM) and powder X-ray diffraction (PXRD) studies confirm the low crystallinity of the samples (see Figure 4 and the Supporting Information, SI-2b and SI-2c). According to UV/Vis spectra, the as-prepared tin-rich ITO films show a transmittance of 85% (see the Supporting Information, SI-4b). Electrical characterization of the tin-rich ITO films by four-point probe measurements at room temperature revealed a remarkably low sheet resistivity of 20.15 Ω per square centimeter for the sample prepared at 250 °C and 4.52 Ω per square centimeter for the sample prepared at 400 °C.

Taking the thickness of the films (1 μm, 250 °C vs. 2 μm, 400 °C) into account, the resistivity is on the order of  $9.1 \times 10^{-3}$  Ω cm (tin-rich ITO 250 °C) and  $4.1 \times 10^{-3}$  Ω cm (tin-rich ITO 400 °C). Thus, the electrical conductivity is about three times higher than the best performance of similar films produced from commercially available ITO powders<sup>[22]</sup> (see the Supporting Information, SI-3) with much higher (expensive) indium content (99–95%). Moreover, the sheet resistance of our tin-rich ITO films in air is quite stable over time

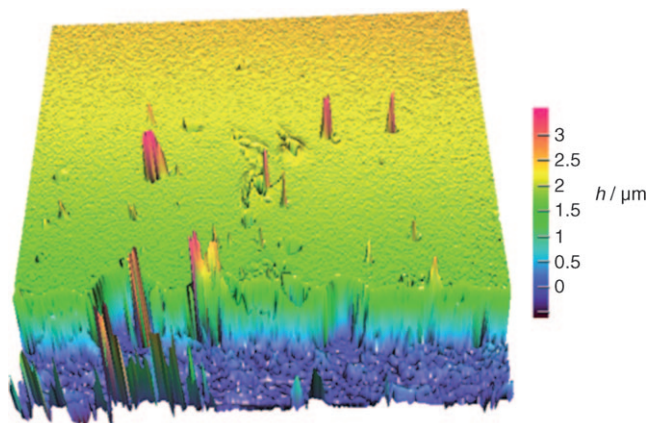


**Figure 2.** Surface topography investigation by confocal microscopy of the as-prepared tin-rich ITO thin film (2 μm) grafted on glass after calcination at 250 °C in dry air.

(see the Supporting Information, SI-5), approaching the performance of a sputtered (crystalline and compact) ITO film. SEM and TEM investigations of tin-rich ITO thin films prepared on top of commercially available ITO-coated glass substrates revealed that in contrast to commercially available ITO, the tin-rich ITO layers maintain their amorphous character even up to 400 °C (see Figure 3 and the Supporting Information, SI-2b and SI-2c). Additionally, using our as-prepared tin-rich ITO film as a transparent conductive electrode, an electroluminescent (EL) device was fabricated by conventional deposition methods.<sup>[23]</sup>

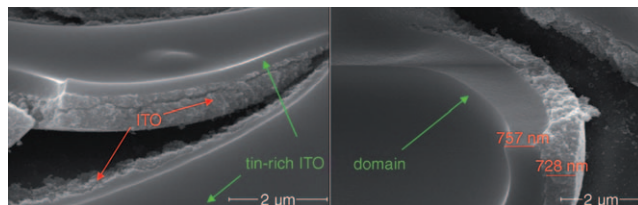


**Figure 3.** Scanning electron microscopy (SEM) images of tin-rich ITO-coated commercial ITO samples prepared at 400 °C in dry air.

The amorphous ITO film on glass was coated with a layer of phosphor (DuPont), then with a dielectric insulating layer, and finally with a silver film. The resulting EL lamp prototype shows a durable high performance with a substantially reduced current consumption up to 50% in comparison to identical EL devices based on commercially available ITO layers (see the Supporting Information, SI-8 and SI-9). Surprisingly, the PXRD patterns of samples recovered from the coating on glass prepared at 250 °C indicate a structure quite similar to the crystalline cubic bixbyite structured In<sub>2</sub>O<sub>3</sub> (ICDD PDF No. 6-416) and elemental β-tin (ICDD PDF No. 4-673; Figure 4).

No indication of other crystalline tin oxides or mixed tin indium oxides could be observed. In agreement with this

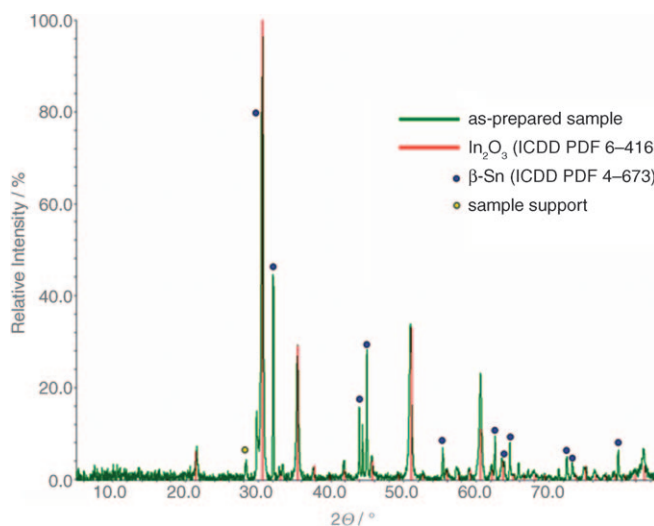


**Figure 4.** X-ray powder diffraction pattern of an as-prepared tin-rich ITO sample recovered from coating on a glass substrate. The sample was prepared by degradation of an ITBO precursor film on glass substrate at 250 °C in dry synthetic air.

finding, the Mössbauer spectrum confirms the formation of elemental tin along with amorphous  $\text{Sn}^{\text{II}}$  and  $\text{Sn}^{\text{IV}}$  oxide species (Figure 5a). Further treatment of the same sample at 400 °C in dry synthetic air leads to complete oxidation of elemental tin to  $\text{Sn}^{\text{IV}}$  and concomitantly little segregation of crystalline  $\text{SnO}_2$ , as confirmed by XRPD analysis and Mössbauer spectroscopy (Figure 5b).

Interestingly, the presence of elemental tin dissolved in the oxide matrix at 250 °C has only a small influence on the optical properties (transmittance) of the films (see the Supporting Information, SI-4) but diminishes their electrical conductivity. In line with this analysis, the electrical conductivity of the tin-rich ITO films increases after oxidative treatment at 400 °C with complete oxidation of  $\text{Sn}^0$  to  $\text{Sn}^{\text{IV}}$ , presumably because the composite is more homogeneous. Remarkably, the overall molar Sn/In ratio of 1:1 in the ITBO precursor is retained in the solids, as shown by energy-dispersive X-ray spectroscopy (EDX with an X-ray penetration depth of about 3–5 nm) and X-ray photoelectron spectroscopy, which indicate no signs of metal loss by sublimation (see the Supporting Information, SI-2b and SI-6).

In other words, the samples are solid solutions of crystalline ITO particles dissolved in an amorphous tin-rich

indium oxide matrix with an overall high atomic dispersion of tin and indium. Apparently, the amorphous character is essential for the relatively high conductivity and good performance of the tin-rich ITO films, because prolonged calcination of samples at 400 °C decreases the conductivity by 30 % owing to crystallization and segregation processes. What could explain the remarkably high stability and conductivity of the mostly amorphous tin-rich ITO composite that prevents tin from forming a segregate tin oxide phase up to 400 °C?

It seems that the presence of tin atoms in different valence states is responsible for the striking properties. In fact, this conclusion is supported by Mössbauer spectroscopy, which shows the presence of approximately 54 %  $\text{Sn}^{\text{IV}}$  (isomer shift  $\delta = 0.12$ ) with little quadrupole splitting as well as approximately 26 %  $\text{Sn}^0$  ( $\delta = 1.98$ ) and 20 %  $\text{Sn}^{\text{II}}$  sites ( $\delta = 3.91$ ) in the amorphous tin-rich ITO composites (Figure 5a). The spectrum of this composite is drastically different from that observed for common ITO phases with varying tin content up to 9 % and/or containing the rhombohedral  $\text{In}_4\text{Sn}_3\text{O}_{12}$  phase.<sup>[11]</sup> Calcination of the tin-rich ITO composite at 400 °C in air leads concomitantly to complete oxidation of  $\text{Sn}^0$  and  $\text{Sn}^{\text{II}}$  to  $\text{Sn}^{\text{IV}}$ , as shown by an increase of the resonance signal of  $\text{Sn}^{\text{IV}}$  sites at the expense of the intensities of the  $\text{Sn}^{\text{II}}$  sites (Figure 5b). The complete conversion of the tin atoms into  $\text{Sn}^{\text{IV}}$  sites may promote higher solubility of ITO particles in tin-rich indium tin oxide but at the same time facilitate crystallization and phase separation. This behavior explains the significant decrease in conductivity of samples calcined for long periods of time.

In summary, the first remarkably stable and highly conductive tin-rich ITO composites have been prepared at 250 °C using the molecular single-source precursor ITBO. The as-prepared transparent and highly conductive tin-rich ITO thin films on glass substrates are mostly amorphous and show an unprecedented long-term stability and high optoelectronic performance in energy-saving EL devices. Intriguingly, the presence of tin atoms in different valence states prevents tin from forming a segregate tin oxide phase up to 400 °C. Taking advantage of this chemical trick, that is, the presence of the same metal species in different oxidation states in solid solutions, could pave the way to novel remarkably stable amorphous multinary TCOs that are cheaper and even more efficient than ITO. Investigations in this area are currently underway.

### Experimental Section

All manipulations involving air-sensitive compounds were carried out in dry, oxygen-free solvents under an inert atmosphere of nitrogen using standard Schlenk techniques. The NMR spectra were recorded on Bruker ARX 200 (1H 200 MHz,  $^{13}\text{C}$  50 MHz) and ARX 400 (1H 400 MHz,  $^{13}\text{C}$  100.64 MHz,  $^{119}\text{Sn}$  149.21 MHz) spectrometers at ambient temperature. Chemical shifts are reported in ppm and referenced to the  $^{13}\text{C}$  and residual  $^1\text{H}$  signals of the deuterated solvents. Chemical shifts for  $^{119}\text{Sn}$  are given relative to  $(\text{CH}_3)_4\text{Sn}$ . Elemental analyses were performed on a Perkin–Elmer Series II CHNS/O Analyzer 2400. Hexamethyldisilazane ( $\text{C}_6\text{H}_{19}\text{NSi}_2$ ) and  $\text{SnCl}_4$  were distilled prior to use. Anhydrous  $\text{SnCl}_2$ , In,  $\text{Br}_2$ , and  $n\text{-BuLi}$  were used as purchased.  $\text{InBr}_3$ ,<sup>[17]</sup>  $\text{LiN}(\text{Si}(\text{CH}_3)_3)_2$ ,  $\text{Sn}(\text{N}(\text{Si}(\text{CH}_3)_3)_2)_2$  were used as purchased.

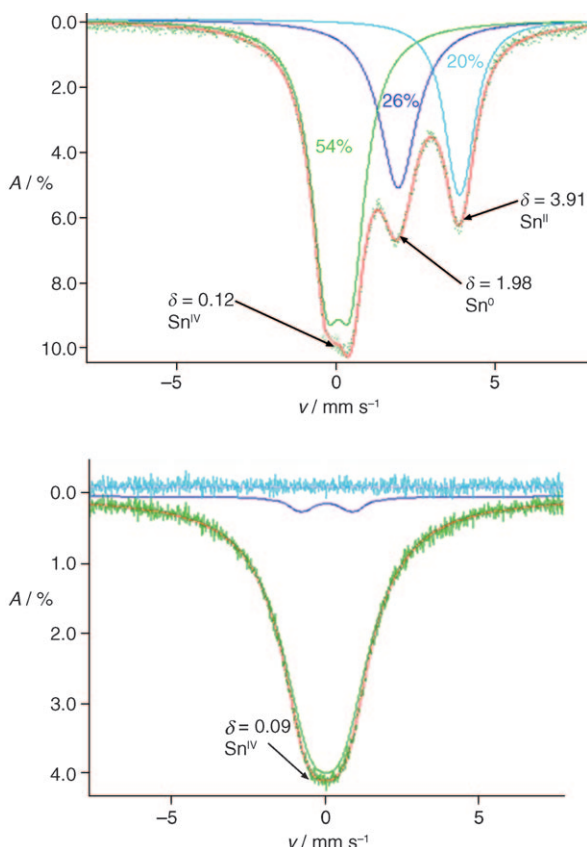


**Figure 5.** Mössbauer spectra of tin-rich ITO samples: a) Sample with tin in different valence states recovered from the coating on glass prepared from the degradation of the precursor ITBO at 250 °C in dry synthetic air; the observed spectrum is shown in red, and simulation curves are displayed above in green and blue. b) The same sample after calcination for 6 h in dry air at 400 °C. The observed spectrum is shown in green and simulation curves are displayed in red and dark blue. The light-blue curve shows the background.

$(\text{CH}_3)_3)_2$ ,<sup>[18]</sup>  $\text{Sn}(\text{OrBu})_2$ ,<sup>[19]</sup>  $\text{NaOBU}$ , and  $\text{Na}(\text{OrBu})_3\text{Sn}$ <sup>[20]</sup> were prepared according to published procedures.

Synthesis of ITBO:  $\text{Sn}(\text{OrBu})_3\text{In}$  (ITBO) was prepared according to a modified literature procedure.<sup>[16]</sup>  $\text{InBr}$  (2.92 g, 15 mmol) was suspended in toluene (100 mL) with anhydrous  $N,N,N',N'$ -tetraethylenediamine (5 drops), and the mixture was stirred 0.5 h at ambient temperature. Subsequently, a concentrated solution of  $\text{Na}(\text{OrBu})_3\text{Sn}$  (3.61 g, 10 mmol) in toluene was added slowly under vigorous stirring, and the reaction mixture was stirred 24 h at 100 °C. After cooling to room temperature, insoluble by-product salts were removed by filtration. Removal of the solvent from the filtrate in vacuo ( $10^{-2}$  mbar) led to the desired product as a pale yellow solid (4.30 g, 95 %).  $^1\text{H}$  NMR ( $\text{C}_6\text{D}_6$ , 200.13 MHz):  $\delta = 1.36$  ppm (s, 27H, OC- $(\text{CH}_3)_3$ ).  $^{13}\text{C}\{^1\text{H}\}$  NMR ( $\text{C}_6\text{D}_6$ , 50.32 MHz):  $\delta = 35.04$  (OC $(\text{CH}_3)_3$ ), 72.49 ppm (OC $(\text{CH}_3)_3$ ).  $^{119}\text{Sn}\{^1\text{H}\}$  NMR ( $\text{C}_6\text{D}_6$ , 149.21 MHz):  $\delta = -78.10$  ppm. Elemental analysis calcd for  $\text{C}_{12}\text{H}_{27}\text{InO}_3\text{Sn}$  (452.87 g mol<sup>-1</sup>): C 31.83, H 6.01 %. Found: C 31.37, H 5.91 %.

Thermogravimetric analysis of the ITBO precursor was carried out with a thermogravimetric setup from Rubotherm under synthetic air (20 %  $\text{O}_2$ , 80 %  $\text{N}_2$ ) with a heating rate of 1 K min<sup>-1</sup>.

X-ray powder diffractograms were recorded with a Bruker-AXS D8 Advance diffractometer using  $\text{CuK}\alpha$  radiation ( $\lambda = 1.5418$  Å) and with a position-sensitive detector (PSD) diffractometer using  $\text{CuK}\alpha$  radiation in the  $2\theta$  range from 25° to 85° with 0.015° steps. Samples were prepared for PXRD measurements by dispersing the sample (ca. 15 mg) in acetone and then applying the dispersion onto a silicon slide and allowing it to dry in air. UV/Vis spectra were recorded using a Perkin-Elmer Lambda 20 spectrometer equipped with a reflecting sphere, Labsphere RSA-PE-20.

Scanning electron microscopy (SEM) images were acquired using a Hitachi S-4000 microscope equipped with an SAMX EDX detector.

Energy-dispersive X-ray spectroscopy using a CAMECA Camebax microbeam electron microprobe was employed to determine the quantitative chemical composition of the particles with a sample current of 18 nA at 15 kV.

Photoemission (XPS) experiments were performed at the end station SurICat (beamline PM4) at the synchrotron light source BESSY in Berlin. The ultrahigh-vacuum (UHV) system consisted of interconnected sample preparation and analysis chambers; base pressure:  $2 \times 10^{-10}$  mbar. Sample transfer between chambers proceeded without breaking UHV conditions. The excitation energies for ultraviolet photoelectron spectroscopy (UPS) and XPS were 630 and 1400 eV, respectively. Photoemission spectra were collected with a hemispherical electron energy analyzer (Scienta SES) under normal emission; the size of the synchrotron spot was set to 1 mm.

The  $^{119}\text{Sn}$  Mössbauer spectra were recorded at 295 K on a CM 2201 spectrometer in constant-acceleration mode. Computer simulation was used to determine isomer shift (i.s.) and quadrupole splitting (q.s.) values. The i.s. values are referenced to  $\text{SnO}_2$ .

Transmission electron microscopy (TEM) was performed on an FEI Sirion microscope operating at 10 keV. The 2D and 3D topographic investigations of the films were accomplished with a Nano-Focus  $\mu\text{Surf}$  confocal microscope. The structure, morphology, and surface conductivity of the coatings were studied with atomic force microscopy using a commercial AFM Nanoscope III-Dimension 3100 instrument (Veeco Instruments).

Four-point probe measurements: The electrical resistivities were measured using the four-point probe method at room temperature, for which the instrument was assembled using a Keithley nanovoltmeter and a Keithley 2400 constant-current source.

Film preparation:  $\text{Sn}(\text{OrBu})_3\text{In}$  (ITBO) was dissolved in toluene to obtain a concentrated solution, which was then spin-coated on glass substrates in a glove box and subsequently heat-treated in dry air atmosphere at different temperatures between 200 and 400 °C. After heat treatment, all samples were annealed at their corresponding drying temperature in a reductive gas mixture of 10 %  $\text{H}_2$  and 90 %  $\text{N}_2$ .

The EL device was fabricated by conventional screen printing methods.<sup>[23]</sup> The conductive and transparent tin-rich ITO layer on glass substrate was coated with a layer of phosphor (DuPont), then with a dielectric insulating layer, and a finally with a silver film. The device was dried for 15 min at 120 °C after each coating. The printing of the dielectric insulator was repeated three times to achieve a suitable layer thickness.

Received: March 3, 2009

Revised: April 29, 2009

Published online: July 7, 2009

**Keywords:** composites · luminescence · molecular precursors · thin films

- [1] K. L. Chopra, S. Major, D. K. Pandya, *Thin Solid Films* **1983**, 102, 1.
- [2] H. Ohta, H. Hosono, *Mater. Today* **2004**, 6, 42.
- [3] a) R. X. Wang, A. B. Djuricic, C. D. Beling, S. Fung, *Trends Semicond. Res.* **2005**, 137; b) D. S. Ginsley, C. Bright, *MRS Bull.* **2000**, 25, 15.
- [4] a) J. Ni, H. Yan, A. Wang, Y. Yang, C. L. Stern, A. W. Metz, S. Jin, L. Wang, T. J. Marks, J. R. Ireland, C. R. Kannewurf, *J. Am. Chem. Soc.* **2005**, 127, 5613; b) P. Canhola, N. Martins, L. Raniero, S. Pereira, E. Fortunato, I. Ferreira, R. Martins, *Thin Solid Films* **2005**, 487, 271.
- [5] J. Ba, D. F. Rohlfing, A. Feldhoff, T. Brezesinski, I. Djerdj, M. Wark, M. Niederberger, *Chem. Mater.* **2006**, 18, 2848.
- [6] G. Bühler, D. Thölmann, C. Feldmann, *Adv. Mater.* **2007**, 19, 2224.
- [7] M. Epifani, R. Diaz, J. Arbiol, P. Sciciliano, J. R. Morante, *Chem. Mater.* **2006**, 18, 840.
- [8] H. Han, D. Adams, J. W. Mayer, T. L. Alford, *J. Appl. Phys.* **2005**, 98, 083705.
- [9] D. Lin, H. Wu, W. Pan, *Adv. Mater.* **2007**, 19, 3968.
- [10] G. Frank, H. Köstlin, *J. Appl. Phys. A* **1982**, 27, 197.
- [11] N. Nadaud, N. Lequeux, M. Nanot, *J. Solid State Chem.* **1998**, 135, 140.
- [12] S. Polarz, A. V. Orlov, M. W. E. Van den Berg, M. Driess, *Angew. Chem.* **2005**, 117, 8104; *Angew. Chem. Int. Ed.* **2005**, 44, 7892.
- [13] a) S. Polarz, A. Roy, M. Merz, S. Halm, D. Schröder, L. Schneider, G. Bacher, F. E. Kruis, M. Driess, *Small* **2005**, 1, 540; b) S. Jana, Y. Aksu, M. Driess, *Dalton Trans.* **2009**, 1516.
- [14] A. Orlov, A. Roy, M. Lehmann, M. Driess, S. Polarz, *J. Am. Chem. Soc.* **2007**, 129, 371.
- [15] Y. Aksu, M. Driess, T. Lütthge, R. Fügemann, M. Inhester, International Patent Application WO PCT/EP2008/050997, **2008**.
- [16] M. Veith, K. Kunze, *Angew. Chem.* **1991**, 103, 92; *Angew. Chem. Int. Ed. Engl.* **1991**, 30, 95.
- [17] V. W. Morawietz, H. Morawietz, G. Brauer, *Z. Anorg. Allg. Chem.* **1962**, 316, 220.
- [18] A. Herve, A. L. Rodriguez, E. Fouquet, *J. Org. Chem.* **2005**, 70, 1953.
- [19] M. Veith, F. Töllner, *J. Organomet. Chem.* **1983**, 246, 219.
- [20] T. Athar, R. Bohra, R. C. Mehrota, *Synth. React. Inorg. Met.-Org. Chem.* **1989**, 19(2), 195.
- [21] K. Zhang, F. Zhu, C. H. A. Huan, *Thin Solid Films* **2000**, 376, 255.
- [22] G. Guenther, G. Schierring, R. Theissmann, R. Kruk, R. Schmechel, C. Baecht, A. Prodi-Schwab, *J. Appl. Phys.* **2008**, 104, 034501.
- [23] [http://www2.dupont.com/MCM/en\\_US/PDF/teachpapers/ELPAPER.pdf](http://www2.dupont.com/MCM/en_US/PDF/teachpapers/ELPAPER.pdf); <http://www.fizyka.umk.pl/~lab2/manual/33/lux-printguide.pdf>.